

Using proteomics and network analysis to elucidate the consequences of synaptic protein oxidation in a PS1+A β PP mouse model of Alzheimer's disease

Brian A. Soreghan^{a,b,*}, Bing-Wen Lu^c, Stefani N. Thomas^{a,*}, Karen Duff^d, Eugene A. Rakhmatulin^e, Tatiana Nikolskaya^e, Ting Chen^c and Austin J. Yang^{a,**}

^a*Department of Pharmaceutical Sciences, University of Southern California, Los Angeles, California 90033*

^b*Research Center for Alcoholic Liver and Pancreatic Diseases, University of Southern California, Los Angeles, California 90033*

^c*Department of Computational and Molecular Biology, University of Southern California, Los Angeles, California 90089*

^d*Center for Dementia Research, Nathan Kline Institute, Orangeburg, New York 12053*

^e*GeneGo, Inc., 500 Renaissance Drive, Suite 106, St. Joseph, Michigan 49085*

Abstract. Increasing evidence suggests that oxidative injury is involved in the pathogenesis of many age-related neurodegenerative disorders, including Alzheimer's disease (AD). Identifying the protein targets of oxidative stress is critical to determine which proteins may be responsible for the neuronal impairments and subsequent cell death that occurs in AD. In this study, we have applied a high-throughput shotgun proteomic approach to identify the targets of protein carbonylation in both aged and PS1+A β PP transgenic mice. However, because of the inherent difficulties associated with proteomic database searching algorithms, several newly developed bioinformatic tools were implemented to ascertain a probability-based discernment between correct protein assignments and false identifications to improve the accuracy of protein identification. Assigning a probability to each identified peptide/protein allows one to objectively monitor the expression and relative abundance of particular proteins from diverse samples, including tissue from transgenic mice of mixed genetic backgrounds. This robust bioinformatic approach also permits the comparison of proteomic data generated by different laboratories since it is instrument- and database-independent. Applying these statistical models to our initial studies, we detected a total of 117 oxidatively modified (carbonylated) proteins, 59 of which were specifically associated with PS1+A β PP mice. Pathways and network component analyses suggest that there are three major protein networks that could be potentially altered in PS1+A β PP mice as a result of oxidative modifications. These pathways are 1) iNOS-integrin signaling pathway, 2) CRE/CBP transcription regulation and 3) rab-lyst vesicular trafficking. We believe the results of these studies will help establish an initial AD database of oxidatively modified proteins and provide a foundation for the design of future hypothesis driven research in the areas of aging and neurodegeneration.

Keywords: Abbreviations: AD, Alzheimer's disease; CRE, cAMP response element; CBP, CREB binding protein; CREB, cAMP response element binding protein; GFAP, glial fibrillary acidic protein; GO, gene ontology; HNE, 4-hydroxynonenol; IL-1 β , interleukin-1beta; iNOS, inducible nitric oxide synthase; LC-MS/MS, liquid chromatography tandem mass spectrometry; MS, mass spectrometry; NFT, neurofibrillary tangles; NO, nitric oxide; NO₃⁻, peroxynitrite; PHF, paired helical filaments; ROS, reactive oxygen species; TNF, tumor necrosis factor.

*These authors contributed equally to this work.

**Corresponding author: Austin Yang, Ph.D., University of Southern California, School of Pharmacy, Department of Pharmaceutical

Sciences, Los Angeles, CA 90089. Tel.: +323 442 4118; E-mail: austiny@usc.edu.

1. Introduction

Alzheimer's disease is a progressive, degenerative disorder of the brain and is the most common form of dementia of the elderly. Upon post-mortem analyses of brain tissue from patients, AD is histopathologically characterized by senile A β plaques, neurofibrillary tangles, and dystrophic neurites. Prominent behavioral manifestations of AD include memory impairments and cognitive decline.

There is an increasing amount of evidence which suggests that oxidative damage has more than an associative role in AD, as well as in aging in general, and that reactive oxygen species (ROS) may be key mediators in the pathogenesis of AD and other neurodegenerative diseases [22,32,33,46]. Extensive oxidative damage has been reported in the brain of AD patients: protein oxidation [37,39], lipid peroxidation [25,35], advanced glycation end products [38], and oxidation of nucleic acids [31]. In fact, ROS-mediated oxidative modifications of macromolecules are more pronounced in brain areas proximal to those regions containing prominent A β deposition [18]. Although the exact mechanism by which these oxidative insults arise in the progression of this neurodegenerative disease is still unclear, it is critical to identify key proteins and signaling pathways that are damaged by ROS that may give a better understanding of some of the aberrant cellular events that occur in AD and other neurodegenerative disorders.

Although no single transgenic mouse model of AD can completely replicate all aspects of the human disease, they provide excellent models for studying specific pathological events due to the expression of the human mutated genes associated with familial AD. One such model, the PS1+A β PP (presenilin-1M₁₄₆L/amyloid β protein precursor K₆₇₀N, M₆₇₁L) double transgenic mouse model of Alzheimer's disease was generated by Karen Duff's group [19], and the mice have been analyzed extensively by various investigators [8,26]. Markers of oxidative stress and learning deficits can be detected in these mice as early as 6 months of age. The temporal relationships between the formation of amyloid aggregates and oxidative damage in the PS1+A β PP transgenic mice suggest that the appearance of A β deposits is tightly associated with the increased accumulation of oxidative markers within these animals [8,26]. Since the PS1+A β PP mouse model clearly replicates some of the most important features of human Alzheimer's disease and age-related oxidative damage, we decided to use these animals in

our studies in an attempt toward our higher goal of establishing a set of oxidatively modified proteins that are specific to these transgenic mice versus age-matched controls to elucidate whether the increased oxidative environment found within AD brain tissue damages or alters key regulatory or signaling proteins involved in neuronal function.

Increased reactive carbonyls were the first form of oxidative damage identified in AD brain tissue [36]; however, the detailed pathological significances of such oxidative modifications remain largely unknown. Carbonylation of proteins is the most widely investigated oxidative protein modification, and the extent of protein carbonylation is often used as a marker to determine the levels of oxidatively-damaged proteins in a biological sample. Using combinations of Oxyblot (a measure of carbonylation), 2-D gel electrophoresis, and mass spectrometric analyses, the identifications of a few of the proteins that are overly-carbonylated in AD brain tissue vs. age-matched controls have only just recently begun to be elucidated within the last couple years. Butterfield's group has been successful in taking this coupled 2-D fingerprinting-immunological detection methodology and subsequent identification of proteins by mass spectrometry to disclose several proteins that are carbonylated in AD brain tissue, including creatine kinase BB, glutamine synthase, ubiquitin carboxy-terminal hydrolase L-1, dihydropyrimidinease-related protein, α -enolase, and heat shock cognate 71 [6,7]. However, because it is known that certain proteins (very basic/acidic proteins, transmembrane proteins, very high molecular weight proteins) are often excluded or unresolved using 2-D gels, we have developed an on-line microcapillary reverse-phase liquid chromatography tandem mass spectrometry (LC-MS/MS) approach coupled with a biocytin hydrazide-streptavidin affinity methodology to enrich for carbonylated proteins [40].

However, the generation of very large numbers (hundreds of thousands) of MS/MS spectra from such high-throughput shotgun proteomic approaches creates a tremendous challenge when correct peptide assignments must be discriminated from false identifications among database search results [21,29]. Aside from the sheer volume of data files that are acquired during such experiments, the raw MS/MS data can be of low quality or have high noise to signal ratios which can further complicate analyses and lead to high false-positive rates of protein identification. Furthermore, of the two most common database search engines (SEQUEST and Mascot) currently used for tandem MS peptide and protein identification, SEQUEST does not

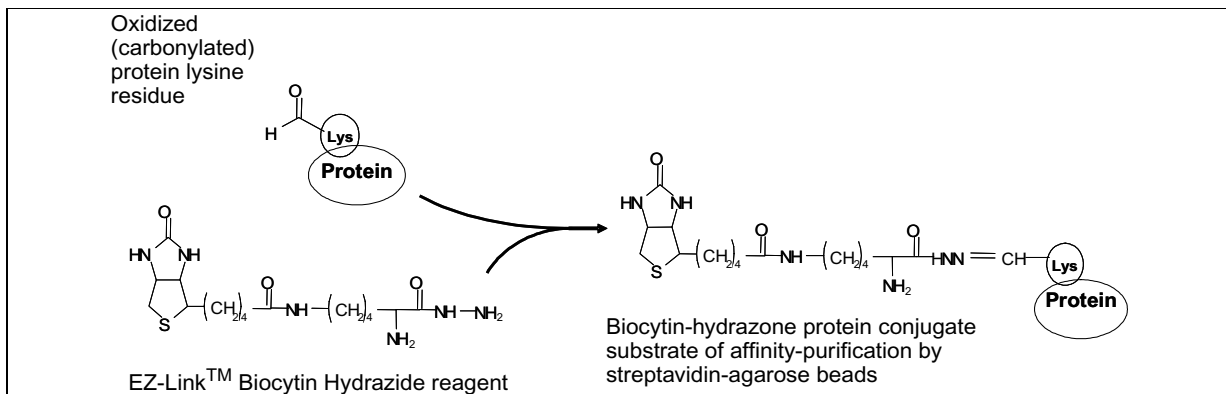


Fig. 1. Reaction of biocytin hydrazide with carbonylated protein.

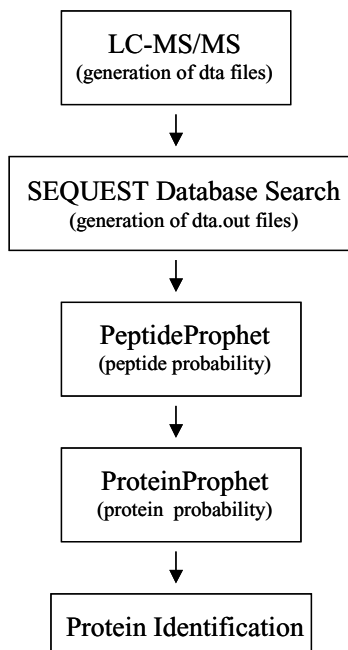


Fig. 2. Workflow of protein identification incorporating data acquisition, the use of SEQUEST (for peptide and protein assignments), PeptideProphet (for the statistical validation of peptide assignments), and ProteinProphet, (for the statistical validation of proteins assigned on the basis of identified peptides).

use a probability-based algorithm, making it difficult to validate peptide assignments. While Mascot does use a probability-based scoring algorithm for assigning MS/MS spectra to peptides, the Mascot scoring scheme is not available to the public, making it less desirable for transparent biological inferences. Since validation of peptide assignments from such search engines by manual inspection of each spectrum from high-throughput experiments is not feasible due to time constraints and/or availability of MS experts, statisti-

cal models, such as PeptideProphet [21] and ProteinProphet [29] have very recently been developed to assess the validity of peptide and protein identifications based on database searches. These automated and robust statistical programs allow for the standardization of data analysis from large-scale proteomic experiments. The fact that PeptideProphet and ProteinProphet are probability-based programs permits the mass spectrometric instrument-, database-, and search engine-independent comparison of data. We have used these mathematical models to analyze our tandem MS data from transgenic and control mice, and we have started to develop a catalog of oxidatively modified (carbonylated) proteins to establish a baseline within the field of oxidation-AD proteomics for the elucidation of potential cellular markers that may be targets of future therapeutic methodologies.

2. Experimental procedures

2.1. Tissue homogenization, protein carbonyl labeling, affinity purification and tryptic digestion

Approximately 50 mg of brain tissue per animal (four transgenic and four 12-month age-matched controls) was cut into small pieces on dry ice and then homogenized essentially as described [40]. The supernatants were separated from the pellets and subsequently reacted with EZ-Link™ biocytin hydrazide (Pierce), and carbonylated proteins were affinity purified using ImmunoPure immobilized streptavidin (Pierce) as described [40]. The proteins were reduced, alkylated, and trypsin treated; tryptic fragments were collected after centrifugation and subsequently lyophilized until analyses by mass spectrometry.

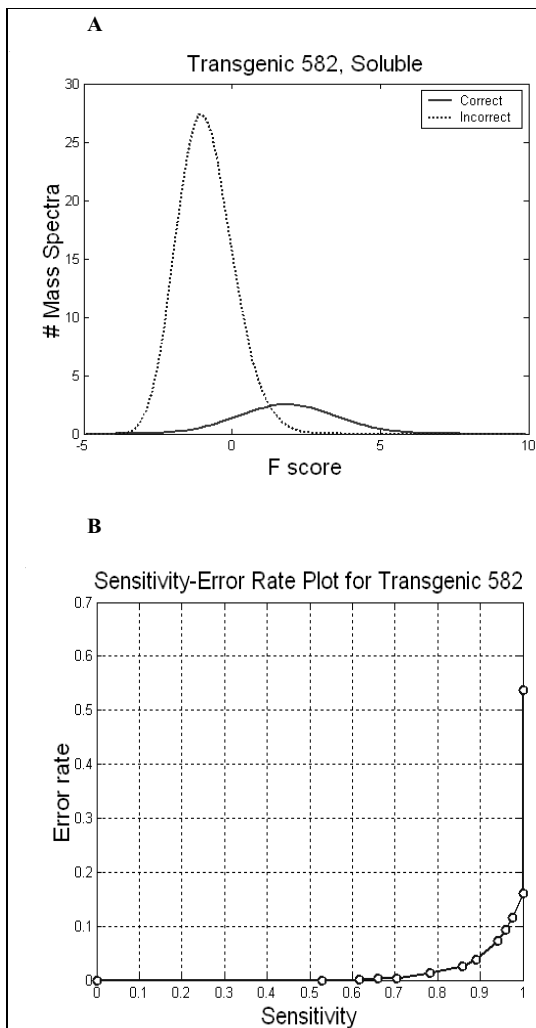


Fig. 3. PeptideProphet and ProteinProphet statistical validation of SEQUEST-generated peptide and protein identifications from one transgenic animal. a) correct and incorrect peptide discriminating scores (F scores) determined by PeptideProphet vs. a portion of the number of mass spectra generated from a typical LC-MS/MS run of mouse brain tissue homogenate, b) ProteinProphet error and sensitivity rates of identified proteins.

2.2. Mass Spectrometry and MS/MS data generation

All samples were analyzed using a Finnigan LCQ Classic ion trap mass spectrometer (Thermo Finnigan, San Jose, CA) using one dimensional liquid chromatography with an Ultra Plus II Proteomic System (Micro-Tech Scientific, Inc., Vista, CA) as previously described [40]. Tandem MS/MS spectra were acquired with Xcalibur 1.2 software, and a new Beta test site version of Bioworks (Bioworks 3.1) on a nine node (2 cpu/node) cluster computer from Thermo Finnigan utilizing the SEQUEST algorithm was used to deter-

mine cross correlation scores between acquired spectra and a mouse protein database [40].

2.3. Validation of peptide assignments and protein inference utilizing PeptideProphet and ProteinProphet

The quality of peptide assignments and protein inference were assessed by using the PeptideProphet and ProteinProphet statistical models detailed in [21,29]. Briefly, PeptideProphet first applies machine learning language to distinguish correct and incorrect peptide assignments from the dataset being analyzed by using an expectation maximization algorithm. The program then computes discriminant scores (F scores) for correct and incorrect peptide assignment using a set of scores generated from SEQUEST search results; this set includes Xcorr (cross-correlation score), ΔC_n (the relative difference between the first and second highest Xcorr score for all peptides queried from the database), SpRank (a measure of how well the assigned peptide scored using a preliminary correlation metric), d_M (the absolute difference between the precursor peptide mass and the assigned peptide) and NTT (number of tryptic termini). Probability scores (p_{comp}) of peptide assignments for each acquired tandem mass spectrum are then calculated based on the distribution of discriminant (F) scores.

These lists of peptide sequences and their respective pcomp scores obtained from PeptideProphet are then used to determine a minimal list of proteins (that are derived from database entries from which the peptide sequences were compared to) that can explain the observed data and to compute a probability (P_{comp}) that each protein is indeed present in the original complex peptide mixture. This is accomplished utilizing the ProteinProphet program that also uses a maximum expectation algorithm similar to PeptideProphet. ProteinProphet uses the following scoring system to determine the probability that a protein is present in a specific sample: 1) NTT: number of tryptic termini (NTT = 0, 1, 2), 2) NSP: number of sibling peptides (different peptide sequences matching the same protein identification), 3) TOT: number of MS/MS spectra matching the same peptide, and 4) peptide probability score (p_{comp}). After analyses, the probability of each protein is then ranked from 0 (incorrect) to 1 (correct). Proteins that are represented by numerous peptides, high percentage sequence coverage, or extremely strong single ion elution profiles are then retained. The final outcome of our analyses (Table 1) was the result of combining all four transgenic animal .dta files into one pool and all four control animal .dta files into another pool.

Table 1
Carbonylated proteins detected in PS1+A β PP transgenic and age-matched control mice, grouped by functional categories

Probability*	Metabolism
1	NP_031477 solute carrier family 25, member 5; adenine nucleotide translocator 2, fibroblast; adenine nucleotide translocase
0.97	NP_062610 TBC1 domain family, member 1; tbc1; tre-2/USP6, BUB2, cdc16) domain family, member 1
0.91	S40961 heterogeneous ribonuclear particle protein A2/B1 – mouse (fragments)
0.90	Q9QZD8 mitochondrial dicarboxylate carrier
0.85	Q61193 Ral guanine nucleotide dissociation stimulator-like 2 (RalGDS-like factor)
0.81	NP_291085 ubiquitin carboxyl-terminal esterase L4
0.63	NP_038848 hexokinase 2
0.51	Q61409 cGMP-inhibited 3',5'-cyclic phosphodiesterase B (Cyclic GMP inhibited phosphodiesterase B) (CGI-PDE B) (CGIPDE1)
0.99/1	Q9Z219 Succinyl-CoA ligase [ADP-forming] beta-chain, mitochondrial precursor (Succinyl-CoA synthetase, beta A chain) (SCS-betaA) (ATP-specific succinyl-CoA synthetase beta subunit)
1/0.99	NP_034053 cyclic nucleotide phosphodiesterase 1
0.88	S39494 glutathione-disulfide reductase – mouse (fragment)
0.86	NP_034133 cytochrome P450, family 2, subfamily c, polypeptide 39; cytochrome P450, 2c39
0.72	NP_112506 chromosome 20 open reading frame 18 isoform 2; HBV associated factor; likely ortholog of mouse ubiquitin conjugating enzyme 7 interacting protein 3
0.62	Q9R1E6 ectonucleotide pyrophosphatase/phosphodiesterase 2 (E-NPP 2) (Phosphodiesterase I/nucleotide pyrophosphatase 2) (Phosphodiesterase I alpha) (PD-Ialpha)
0.55	P09838 DNA nucleotidyltransferase (Terminal addition enzyme) (Terminal deoxynucleotidyltransferase) (TDT) (Terminal transferase)
0.53	NP_033256 sterol O-acyltransferase 1; adrenocortical lipid depletion
0.52	NP_033799 amylase 2, pancreatic
0.51	Q9JHW4 selenocysteine-specific elongation factor (Elongation factor sec) (mSelB)
	Signaling proteins
1	P11798 calcium/calmodulin-dependent protein kinase type II alpha chain (CaM-kinase II alpha chain) (CaM kinase II alpha subunit) (CaMK-II alpha subunit)
0.91	NP_071311 salvador homolog 1; WW domain-containing protein 3; WW domain-containing protein 4
0.79	P21275 bone morphogenetic protein 4 precursor (BMP-4) (BMP-2B)
0.59	NP_034380 gamma-aminobutyric acid (GABA-A) receptor, subunit alpha 1
0.57	Q60934 glutamate receptor, ionotropic kainate 1 precursor (glutamate receptor 5) (GluR-5) (GluR5)
0.67/1	JG0193 G protein-coupled receptor FEX
1	NP_652762 diphtheria toxin resistance protein required for diphthamide biosynthesis
1	NP_036081 mitogen activated protein kinase 14; cytokine suppressive anti-inflammatory drug binding protein 1; p38 MAP kinase
0.99	NP_035340 protein tyrosine phosphatase, receptor type, C
0.98	NP_067433 frizzled 3
0.93	NP_038688 sema domain, immunoglobulin domain (Ig), transmembrane domain (TM) and short cytoplasmic domain, (semaphorin) 4D; M-sema G; semaphorin H
0.90	S58032 probable olfactory receptor tpcr51
0.86	S04743 TPA-induced protein 11
0.85	S71625 protein-tyrosine-phosphatase, nonreceptor type 13
0.80	NP_067307 glucagon-like peptide 1 receptor
0.73	NP_150086 nerve growth factor receptor (TNFR superfamily, member 16); p75 neurotrophin receptor
0.70	O88879 apoptotic protease activating factor 1 (Apaf-1)
0.67	I56335 apolipoprotein J
0.66	NP_035777 tuberous sclerosis 2
0.61	NP_031635 caspase 4, apoptosis-related cysteine protease; caspase 11
0.50	JE0236 tissue kallikrein
	Inflammatory related proteins
1	NP_031598 complement component 1, q subcomponent, alpha polypeptide
0.98	Q00651 integrin alpha-4 precursor (integrin alpha-IV) (VLA-4) (CD49d)
0.97	I54100 lymphocyte antigen – mouse (fragment)
0.87	NP_003802 tumor necrosis factor (ligand) superfamily, member 9; receptor 4-1BB ligand; homolog of mouse 4-1BB-L
0.86	NP_035057 nitric oxide synthase 2, inducible, macrophage
0.83	P24063 integrin alpha-L precursor (leukocyte adhesion glycoprotein LFA-1 alpha chain) (Leukocyte function associated molecule 1, alpha chain) (CD11a)
0.64	P08103 tyrosine-protein kinase HCK (p56-HCK/p59-HCK) (Hemopoietic cell kinase) (B-cell/myeloid kinase) (BMK)
0.62	Q62190 macrophage-stimulating protein receptor precursor (MSP receptor) (p185-Ron)
0.60	P30204 macrophage scavenger receptor types I and II (Macrophage acetylated LDL receptor I and II) (Scavenger receptor type A) (SR-A)

Table 1, continued

Probability*	Metabolism
0.56	NP_058624 toll-like receptor 5
1/1	NP_031600 complement component 1, q subcomponent, gamma polypeptide; complement component 1, q subcomponent, c polypeptide
0.63	NP_034869 lymphocyte antigen 64
	Structural proteins
1	Q61554 Fibrillin 1 precursor
1	NP_006079 tubulin, beta, 2
0.99	VEMSGF glial fibrillary acidic protein, astrocyte
0.97	JC5963 stable tubule only polypeptide
0.96/0.61	MBMSB golli-myelin basic protein precursor
1/1	S53793 actin – mouse (fragments).
1/1	NP_001092 beta actin; beta cytoskeletal actin
1/1	NP_059075 tubulin, alpha 8; tubulin alpha 8
0.97/1	P05213 tubulin alpha-2 chain (Alpha-tubulin 2)
1/1	NP_006078 tubulin, beta, 5
1/1	B25819 actin, fetal skeletal/adult cardiac muscle – mouse (fragment)
1/1	P08551 neurofilament triplet L protein (68 kDa neurofilament protein) (Neurofilament light polypeptide) (NF-L)
0.87/0.99	Q9QYR6 microtubule-associated protein 1A (MAP 1A)
1	NP_034311 fibrillin 2; syndatyls ems [Mus musculus]
0.99	B25437 tubulin beta-2 chain – mouse (fragment)
0.97	Q9Z2Q5 39S ribosomal protein L40, mitochondrial precursor (L40mt) (MRP-40)
0.81	NP_032018 fibulin 2
	Transcription factors/DNA binding proteins
1	NP_032275 transcription factor B2, mitochondrial; house-keeping protein
1	PC7085 nuclear factor of activated T cell, Rel type domain containing protein, NFATz2
1	Q64127 transcription intermediary factor 1-alpha (TIF1-alpha) (Tripartite motif protein 24)
1	P45481 CREB-binding protein
0.98	A47392 chromodomain-helicase-DNA-binding protein, CHD-1
0.95	NP_032261 hairy and enhancer of split 1; hairy and enhancer of split 1
0.91	O54956 DNA Polymerase epsilon subunit B (DNA Polymerase II Subunit B)
0.72	NP_004417 polyhomeotic 1-like; early development regulator 1; mouse Rae28-like
0.66	AAH17556 Rb1-inducible coiled coil protein 1
0.57	NP_034013 CCAAT/enhancer binding protein beta; C/EBP BETA; nuclear protein I16
0.54	NP_444432 forkhead box P1
0.51	Q64092 transcription factor E3
0.50	P55200 zinc finger protein HRX (ALL-1)
0.80/0.91	Q9JK30 origin recognition complex subunit 3 (origin recognition complex subunit Latheo)
0.93/1	Q99MZ3 Williams-Beuren syndrome chromosome region 14 protein homolog (Mlx interactor)
0.79	NP_031986 ets variant gene 1; ets related protein 81
0.77	A25472 homeotic protein Hox A5 – mouse (fragment)
0.75	NP_075779 makorin, ring finger protein, 2; Makorin RING zinc-finger protein
	Trafficking/organelle movement
1	NP_015499 defective in vacuolar protein sorting; homologous to mouse SKD1 and to human hVPS4;
0.99	S55261 myosin heavy chain, dilute – mouse (fragment)
0.98	O08638 myosin heavy chain, smooth muscle isoform (SMMHC)
0.97	NP_034878 lysosomal trafficking regulator
0.86	NP_001650 ADP-ribosylation factor 3
0.86	NP_001654 ADP-ribosylation factor 6
0.57	NP_033029 RAB4A, member RAS oncogene
0.54	NP_683724 transformed mouse 3T3 cell double minute 1
0.51	NP_444307 membrane associated transporter protein; underwhite; B/AIM-1-like protein; dominant brown
1	NP_075373 vacuolar protein sorting 35; maternal embryonic message 3
0.99	NP_038653 platelet-activating factor acetylhydrolase, isoform 1b, beta1 subunit; lissencephaly-1 protein; platelet-activating factor acetylhydrolase 1B alpha subunit
0.86	NP_444299 autophagy 5-like
	Channels/transporters
1	P59158 solute carrier family 12 member 3 (Thiazide-sensitive sodium-chloride cotransporter) (Na-Cl symporter)
0.67	NP_036059 chloride channel 6
0.86	O35219 potassium voltage-gated channel subfamily H member 2 (Ether-a-go-go related gene potassium channel 1) (ERG1) (MERG) (Merg1) (Eag related protein 1)
0.70	NP_032460 potassium voltage-gated channel, subfamily Q, member 1

Table 1, continued

Probability*	Metabolism
	Cell-cell interactors
0.80	P02469 laminin beta-1 chain precursor (laminin B1 chain)
0.64	NP_075538 calyntenin 1; calyntenin-1
0.51	PN0510 integrin beta-3 chain – mouse (fragment)
1	NP_033996 cadherin 11; OB-cadherin; osteoblast-cadherin
0.78	XP_147222 claudin 5
	Development
0.76	NP_065620 otoraplin
0.55	Q05859 formin 1 isoform IV (Limb deformity protein)
0.62	NP_034023 chordin
0.58	P35803 neuronal membrane glycoprotein M6-b (M6b)
	Other
0.82	P21447 multidrug resistance protein 3 (P-glycoprotein 3) (MDR1A)
0.51	NP_033746 a disintegrin and metalloprotease domain 19 (meltrin beta); meltrin beta
0.69	NP_035911 a disintegrin and metalloprotease domain 25
	Unknown
0.87/0.84	<i>P58742 aladin (adralalin)</i>
0.86	Q8K031 StAR-related lipid transfer protein 8 (StARD8) (START domain-containing protein 8)

*Probability (P) of correct protein assignment was determined by ProteinProphet and all proteins have protein probability value > 0.5 as described in Experimental Procedures. Proteins in bold are specific to PS1+A β PP transgenic mice; in italics, common to both transgenic and age-matched controls; in normal font, specific to age-matched controls.

3. Results

As increasing evidence has suggested that oxidative damage in brain tissue is intimately related to neurodegeneration and Alzheimer's disease, we undertook an investigation to elucidate proteins that may be specifically oxidatively modified (carbonylated) in AD transgenic mice versus age-matched controls. Traditionally, the identification of protein carbonylation has been through the derivatization of carbonyl groups by 2,4-dinitrophenylhydrazine (DNPH), followed by immunostaining of DNP conjugated proteins with anti-DNP antibody. The identifications of DNP-modified carbonylated proteins are then subsequently determined by either 2-D gel electrophoresis/immunoblotting analysis or 2-D gel electrophoresis/mass spectrometric analyses. In this study, we utilized our biocytin hydrazide-streptavidin affinity methodology coupled to an LC-MS/MS shotgun proteomics approach that we have previously applied to brain tissue from aged mice [40]. A schematic representation of the chemistry involved in the reaction of biocytin hydrazide with carbonylated proteins is presented in Fig. 1. However, in this case, we incorporated the use of statistical models, PeptideProphet and ProteinProphet, to validate our protein identifications and to circumvent the listings of hundreds of proteins, the majority of which could very well be misassignments. The generation of very large numbers of MS/MS spectra from such high-throughput shotgun proteomic approaches has created a tremendous challenge in deciphering correct protein

assignments from falsely identified ones using protein database searching algorithms as discussed previously [21,29].

The integration of our statistical validation of protein identification with respect to our proteomic approach is shown schematically in Fig. 2. As in our last study [40] tandem MS data (.dta files) were acquired with a Finnigan ion trap mass spectrometer and analyzed using a new Beta test site version of Bioworks (version 3.1) from Thermo Finnigan utilizing the SEQUEST algorithm to determine cross correlation scores between acquired spectra and a mouse protein database. SEQUEST database search results (.out files) were then subjected to a statistical data analysis using the computer program, PeptideProphet [21]. This algorithm uses a set of scores from SEQUEST and creates a set of discrimination (F) scores for all peptides matched by SEQUEST. By using an expectation maximization algorithm, PeptideProphet determines the distribution of both correctly and incorrectly identified peptides within the observed dataset. One example of our transgenic mouse data is shown in Fig. 3(A), which illustrates the distribution of positive and negatively identified peptides using this mathematical model. From Fig. 3(A) it is clear that true positives (correct identifications indicated by the solid line) and false positives (incorrect identifications denoted by the dashed line) have distinct distributions. From these distributions, we can assign a probability score to each identified peptide, giving a measure of confidence in peptide identification. For example, a probability score of 0.9 means we are

90% certain that the identification is correct. The next step in mass spectrometry-based protein identification is the assignment of proteins from which these peptides were derived. The program, ProteinProphet [29], accomplishes this by again computing a probability score (P_{comp}) for each protein potentially identified. A false identification error rate vs. sensitivity (fraction of all correct peptide assignments accepted by the user) can be plotted as shown in Fig. 3(B).

Sensitivity is the percentage of proteins in the sample that are identifiable. Error rate is the percentage of incorrectly identified proteins among total identified proteins. The same data set analyzed by PeptideProphet in Fig. 3(A) was then analyzed by ProteinProphet and the result is depicted in the curve shown in Fig. 3(B). As demonstrated in Fig. 3(B), analysis of our proteomic data yielded 90% sensitivity ($P = 0.90$ as indicated by arrow in Fig. 3B) with an error rate of less than 5%. That is, we have the ability to identify 90% of the proteins in the sample with less than 5% of the proteins being identified as false positives.

The .dta files generated for each of the four transgenic animals were pooled together and then analyzed by these statistical modeling programs. The same was done for each of the four age-matched control animals. The results of the positively identified ($P_{\text{comp}} > 0.5$ from ProteinProphet) proteins of each group are shown in Table 1. For ease of visualization, the proteins were manually compiled into 'functional' categories loosely based on protein function, such as metabolism, signaling, trafficking, proteins involved in immunity/inflammation, structural proteins, etc. Of a total of 117 proteins that were identified from SEQUEST and the statistical models, we found 59 to be specific to the transgenic group (in bold font), 42 specific to the control group (normal font), and 16 that were common to both groups (in italics). Of this last group, 9 of the 16 fell into the structural protein category. Although the time involved in manually separating these proteins into functional categories was not overly-excessive, the amount of time that could be spent on this process would exponentially escalate if further experiments were conducted whereby each animal is to be analyzed separately and/or the number of groups of animals (e.g. other transgenic mouse models of AD) is increased. For this reason, we have recently set up an automated system based upon that at the Incyte Human Proteome Database. Currently, proteins are classified into 42 different cellular processes which are a reflection of the biological process ontology adopted by the *Gene Ontology* (GO) hierar-

chical classification system. A final filter cutoff value ($P_{\text{comp}} > 0.5$) was chosen from ProteinProphet, and the NCBI annotations of the identified proteins were converted to LocusLink IDs using NCBI's LinkOut program. The list of LocusLink IDs was then used as input data by the publicly available GoSurfer (URL: <http://www.biostat.harvard.edu/complab/gosurfer/>) for GO analysis. Finally, all proteins are assigned to one or multiple cellular process categories. An example of this gene annotation analysis is depicted in Fig. 4 which indicates the functional groups of proteins identified from our PS1+A β PP transgenic mice.

In addition, our proteomic datasets were also subjected to more extensive pathway analyses using MetaCoreTM. MetaCoreTM is a program developed and based on Systems Reconstruction technology which contains over 11,500 human pathways (both metabolic and signal transduction), over 12,000 biochemical reactions and more than 250 manually curated maps for major functional pathways of cellular processes [48]. Curation is carried out on two levels. On the first level, experimental data from original scientific publications is used to create individual reactions, short pathways, and signaling interactions. On the second level, larger maps for major functional blocks are assembled from selected review publications. The pathways on these maps are linked into larger functional models/blocks via joint metabolites, signaling proteins and/or regulatory effectors. MetaCoreTM therefore represents an integrated database on human and mammalian signaling, regulatory and metabolic pathways, which are interconnected via associations between genes, proteins, metabolites, pathways and human diseases. These maps and pathway networks represent the backbone for the integration of several types of experimental data, such as mRNA expression, protein expression (for example, from 2D-PAGE or mass spectrometry), protein-protein interaction assays (yeast two-hybrid systems, co-immunoprecipitation), metabolic profiles, and enzymatic activity.

An example of a functional network analysis using MetaCoreTM is shown in Fig. 5, which demonstrates several key signaling pathways comprised of such proteins as inducible nitric oxide synthase (iNOS) and cAMP response element binding protein-binding protein (CBP) that could potentially be altered in PS1+A β PP mice. This observation is consistent with previous reports that both iNOS [9] and CREB [20,24] are critical in maintaining synaptic function, which becomes compromised early in the development of AD pathogenesis. Analysis of the reconstructed protein-

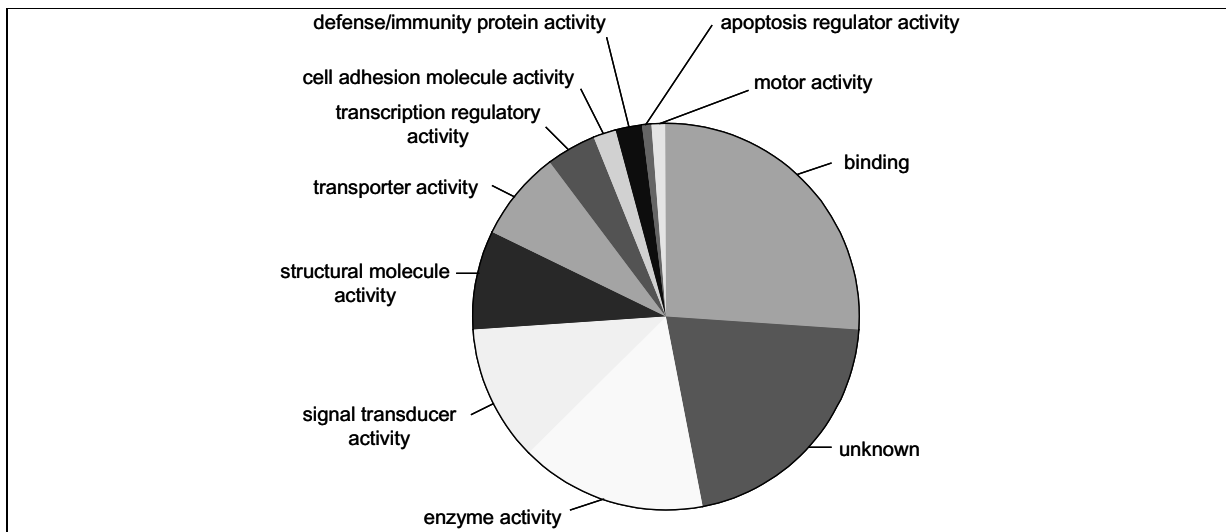


Fig. 4. The NCBI annotations of the identified proteins from PS1+A β PP mice were first converted to LocusLink IDs followed by GO analysis using GoSurfer. The gene annotation analysis of molecular function is then presented as a pie chart. Percent areas are as follows: apoptosis (1%), binding (27%), cell adhesion (2%), defense/immunity protein activity (2%), enzyme activity (16%), signal transduction (11%), structural protein (8%), transporter activity (7%), transcription regulator activity (4%), motor activity (1%) and unknown function (21%).

protein interaction pathway further suggests that signaling pathways involving CREB are among those which may be altered in PS1+A β PP mice. In addition, the pathway analysis also indicates that such defects in CREB signaling could have profound effects on rab-lyst vesicular trafficking. Although the interaction between CREB and rab proteins is largely unknown, systems reconstruction analysis postulates this CREB-rab interaction could be indirectly mediated through a p53-mediated cell signaling pathway. The aforementioned proteins are encircled in Fig. 5. The vectors in Fig. 5 indicate various other protein-protein interactions, thereby facilitating the formation of hypotheses with respect to the potential consequences of protein post-translational modifications, such as carbonylation, which could alter the nature of protein-protein interactions in numerous signaling pathways.

4. Discussion

We have used a rapid and sensitive proteomic analysis coupled with bioinformatic statistical modeling programs to identify carbonylated proteins in brain homogenates of a double transgenic (PS1+A β PP) mouse model of Alzheimer's disease. We utilized an enrichment procedure that we previously developed to detect and identify protein carbonylation events between aged and young mice using a biocytin hydrazide and streptavidin affinity methodology [40]. However, in

this study, we used the computer algorithms, PeptideProphet and ProteinProphet [21,29], to statistically validate our protein identifications from our LC-MS/MS acquisition data sets. Our results showed that we were able to identify 59 proteins unique to the transgenic animal group (4 animals) and 42 proteins specific to the age-matched control group (4 animals). We detected 16 proteins that were found in both groups.

One of the most difficult tasks during the course of this study is to validate the large numbers of spectra that are generated by our shotgun proteomic approach. In particular, correct peptide assignments must be discriminated from false identifications among database search results. Since manual inspection of each spectrum is not feasible due to time constraints, and very often the expertise required to analyze such complex data is not readily available, statistical models, such as PeptideProphet and ProteinProphet, have very recently been developed to assess the validity of peptide and protein identifications based on database searches. The use of such powerful statistical tools can ensure an objective standard with which to interpret our data and the proteomic data from other laboratories.

However, one important caveat to keep in mind is that any mass spectrometry-based protein identification is completely dependent on the sequences that have been deposited into the database. For example, for any peptide sequence, the SEQUESTTM algorithm will only identify the most likely match for a protein in the database. As a result, if a protein does not exist in

flammation and the acute phase response. It has been shown that several key inflammatory proteins can be identified in senile plaques of AD brains. In addition, some of these proteins, such as α 1-antichymotrypsin, α -macroglobulin, apolipoprotein E and heparan sulphate proteoglycan, are also known to promote A β aggregation. In AD, it is well documented that activated astrocytes and microglia, complement pathways and accumulation of proinflammatory cytokines are often tightly associated with amyloid plaques and dystrophic neurites [11]. Therefore, it is widely accepted that activation of inflammatory pathways plays a critical role in the early initiation and propagation of Alzheimer's disease. Immunopathological studies of PS1+A β PP mice have indicated that microglia and astrocytes are activated by both fibrillar and soluble A β and that there is a direct correlation between increased levels of C1q complement proteins and cyclooxygenase-2 expression in response to depositions of fibrillar A β [27]. Our results suggest that various glial markers such as GFAP, C1q and TNF- α receptor are also the targets of oxidative stress. Although the pathological significances of these modifications remain largely unknown at this time, earlier studies have demonstrated that C1q plays an active role in the phagocytosis of A β aggregates by microglia. ROS modification of C1q may enhance C1q-A β interaction and lead to the accumulation of fibrillar A β [27]. It has been shown that C1q-immunoreactivity is specifically associated with thioflavin-S positive fibrillar staining. Although it is not clear whether C1q is oxidatively modified in this study, it has been documented that markers of oxidative stress, such as 4-hydroxynonenol (HNE) and 3-nitrotyrosine, are strongly associated with fibrillar A β in PS1+A β PP mouse brain [26]. The levels of several cytokines, such as IL-1 β [16] and tumor necrosis factor (TNF) [13,15] in AD have also been reported to be increased in AD compared to age-matched controls. We did not observe oxidative modifications of these cytokines; however, our results indicate that various receptors such as the TNF receptor, scavenger receptor and macrophage-stimulating protein receptor (MSP receptor), are the targets of oxidative stress suggesting that alteration of cell signaling and proinflammatory pathways could ultimately lead to brain injury and synaptic dysfunction.

4.2. Oxidation of cytoskeletal proteins

Cytoskeletal proteins, such as β -tubulin and β -actin, have recently been identified as oxidatively modified in

AD by utilizing an immunohistochemical and two dimensional gel electrophoresis analysis [4]. Furthermore, the degrees of protein carbonylation on these cytoskeletal proteins were significantly higher in AD brains than in age-matched control brains, suggesting that there may be a causal relationship between the changes of cytoskeletal protein functions and these oxidative stress related post-translational modifications [4]. In fact, comprehensive biochemical analyses have revealed that modification of neurofibrillary tangles (NFT) by HNE can lead to the cross-linking of NFT and is essential for the initial assembly of paired helical filaments (PHF) suggesting that the oxidative modification of NFT by lipid peroxide, such as HNE, may play an important role in the formation of NFT during the course of Alzheimer's disease [45].

We detected a series of motor proteins, the myosins, which are present specifically in PS1+A β PP mice. Myosin proteins are actin-based motors with a wide variety of functions, including the trafficking and localization of proteins within intracellular compartments. Membrane trafficking events are critical to both pre- and postsynaptic processes, and knowledge of how myosins contribute to these processes will lead to a greater understanding of neuronal function. In the CNS, Myosin V is highly expressed in hippocampal pyramidal cells, localizing both to dendritic spines and shafts, and is an abundant component of the postsynaptic density (PSD) [12,43]. Therefore, one would predict the alteration of myosin function will have a profound effect on both pre- and post-synaptic transport.

4.3. Signaling

Interestingly, several proteins involved in signal transduction and cell signaling have also been identified to be the targets of oxidative stress specifically in PS1+A β PP mice. Calcium (Ca²⁺)/calmodulin-dependent protein kinase (CaMKII) is a multifunctional protein kinase and regulation of CaMKII in hippocampus has been shown to play an important role in neuroplasticity, gene expression, learning, and memory [5,10,14,17,28]. Besides possible alterations in protein phosphorylation, our initial pathway analysis study also suggests that NOS-mediated signaling transduction could be altered in PS1+A β PP mice. Although the roles of nitric oxide (NO) and peroxynitrite (NO₃⁻) in the pathogenesis of AD remain controversial, several recent studies have indicated that iNOS and nitrotyrosine immunoreactivity could be detected in pyramidal-like neurons and glial cells in the brains of AD patients,

suggesting that the modification of proteins by peroxynitrite can be a key factor in the early development of AD [23]. Furthermore, it has been shown *in vitro* that A β is able to stimulate the production of iNOS in cultured astrocytes and that this A β -mediated iNOS induction is at least in part regulated by IL-1 β and TNF- α -dependent cell signaling pathways [3]. Most importantly, the result of our pathway component analysis (Fig. 5) also suggests that there might be a cross-talk between iNOS-mediated cell signaling and CREB-regulated gene expression in PS1+A β PP mice, suggesting that increases in NO-mediated oxidative stress could also lead to changes in CREB mediated gene expression. It is well documented (see [1] for review) that the cyclic-AMP signaling system and CREB-mediated transcription play key roles in the conversion of short- to long-term memory and synaptic plasticity. Therefore, our results suggest that alteration of iNOS and CREB signaling pathways in PS1+A β PP mice could have a profound effect on memory consolidation and the progression of AD pathogenesis.

In addition to being one of the reactants involved in the formation of nitrotyrosine, NO also plays a critical role in cell signaling. As suggested in Fig. 5, the oxidative modifications of integrins such as alpha-4/beta-7, alpha-L/beta-2, alpha-4/beta-1, and alpha-2b/beta-3 integrin could potentially be linked to the perturbation of cell signaling pathways which involve iNOS. Microglial cell activation plays a central role in acute and chronic inflammatory processes associated with neurodegeneration. In a study of activated neonatal rat microglial cells which express integrins such as CD11b (integrin alpha b) and CD29 (integrin beta-1), iNOS activity was found to be increased in addition to a concomitant enhancement in the production of NO [49]. Additionally, in activated macrophages, the activity of iNOS has been found to be associated with integrin-linked kinase (ILK) [42]. Within the context of the reconstructed pathway analysis as presented in Fig. 5, these findings could suggest that oxidative modification of integrins or of iNOS itself could substantially alter the activity of iNOS and subsequently the concentration of NO, hence also altering cell signaling pathways involving the NO and the afore-mentioned proteins.

4.4. Membrane and vesicular trafficking

It is widely documented that abnormalities of the neuronal endocytic pathways are very early markers of Alzheimer's disease [30], and similar endosomal/lysosomal abnormalities have also been reported in

PS1+A β PP mice as well [2]. Although the mechanism leading to these abnormal endocytic pathways in AD is largely unknown, we observed that neurobeachin, also known as lysosomal trafficking regulator, is also a target of oxidative stress in these transgenic mice. It has been shown that neurobeachin displays a high-affinity binding site ($K_d = 10$ nM) for the type II regulatory subunit of protein kinase A (PKA RII) [44]. Subcellular localization studies indicate that neurobeachin is peripherally associated with pleiomorphic tubulovesicular endomembranes near the trans sides of Golgi stacks and throughout the cell body and cell processes. In some cases, neurobeachin has also been observed to concentrate within a subpopulation of the postsynaptic membrane. Genetic analysis of spontaneous neurobeachin insertion mutant mice have indicated that the function of neurobeachin may entail neuron-to-neuron transmission rather than the development of synapses since the differentiation of synapses was completely normal in neurobeachin null mice [41]. Furthermore, we have also identified that a rab-related GTPase is also a target of ROS. However, one should also note that the identification of rab-4 in this study is solely based on a single peptide. This issue becomes critical when a protein is part of a large protein family such as rab. Therefore, our results in this study only suggest that one of the rab family proteins is oxidatively modified rather than rab-4 specifically since we did not observe any MS/MS spectra that are specific for rab-4.

In conclusion, we have used a high throughput proteomics analysis to examine the targets of oxidative damage in a PS1+A β PP mouse model of Alzheimer's disease. By coupling this approach with several newly developed bioinformatics and network analysis tools, we have tentatively identified three major pathways 1) iNOS-integrin signaling pathway, 2) CRE/CBP transcription regulation and 3) rab-lyst vesicular trafficking that could be altered specifically in these animals. Since AD is a progressive disease, the elucidation of the earliest protein targets of oxidation could potentially serve as early markers for the development of early AD diagnosis during the initial processes of neurodegeneration. Given the number of oxidized proteins that were identified as specific to the transgenic mice, 59, and the number of proteins specific to the age-matched control mice, 42, the suitability of the PS1+A β PP mouse as a model of protein oxidation in AD might come into question. To that end, it should be noted that the list of identified proteins (Table 1) is not exhaustive and should serve as a benchmark for more conclusive studies designed to experimentally validate

and more precisely elucidate differences in the classes of proteins which are susceptible to carbonylation in transgenic versus age-matched control mice. We believe the outcomes of the present study will provide an initial baseline from which new hypothesis-driven types of research can be formed in the area of aging and various age-related neurodegenerative diseases.

The degree of reproducibility of this type of bottom-up proteomic analysis, in terms of protein identification, is rather high at the protein level, but in general not at the peptide level. The issue of the reproducibility of protein identification can be addressed from both a bioinformatic stand-point [34], (effectively minimizing the false positive identification rate) as well as from a chromatographic point of view [47] (optimizing the system's dynamic range – ratio of the abundance of highly abundant proteins to low abundance proteins). In the presently described study, the chromatographic method used was optimized and we employed a robust bioinformatic approach in order to achieve high reproducibility at the protein level. The approach used is not a screening method and the proteomic (or mass spectrometry-based protein identification) technology was applied solely to identify the targets of oxidatively modified proteins.

Briefly, eight animals (four PS1+A β PP transgenic mice and four wild type age-matched controls) were used in this study. The reproducibility and probability of protein identification were calculated using the programs PeptideProphet and ProteinProphet which both use an expectation maximization algorithm. In contrast to microarrays, the methods of data processing and validation of shotgun proteomic data analysis are significantly different. In the case of microarray analysis, the known oligonucleotide sequences are laid down on the matrix prior to the experiment, therefore only the expression of pre-determined or known genes can be investigated. However, it should be noted that, in general, the rates of “false hybridization” cannot be determined. As a result, the only way to circumvent the issue of false hybridization is through the analysis of very large numbers of datasets (or slides) as the validation of signal (or hybridization efficiency) from each individual gene within a particular slide (or filter in some cases) is technically unfeasible.

On the other hand, in shotgun proteomics experiments, unknown protein mixtures are typically trypsinized and analyzed via tandem mass spectrometry. Tandem mass spectra are subsequently searched against a protein database and each individual protein is identified using the Sequest algorithm by virtue of the

x-correlation score of the protein's constituent peptides, which is the bioinformatic measurement of the similarity between the theoretical and experimental spectra generated from a given peptide. Hence, the confidence and accuracy of each individual peptide and protein in this study was determined objectively through our bioinformatic approach. We believe the workflow presented in this study could potentially be beneficial for various AD research laboratories, when the independent evaluation of protein identification generated by tandem mass spectrometry is needed. Additionally, the outcomes of the present study will provide an initial baseline from which new hypothesis-driven types of research can be formed in the areas of aging and various age-related neurodegenerative diseases.

Acknowledgements

This work was supported by a grant awarded by the National Institutes of Health (A.Y., MH59786-01) as well as an Alzheimer's Association award (A.Y.). B. S. was supported by the Training Program in Alcoholic Liver and Pancreatic Diseases (T32 AA07578) funded by the National Institute on Alcohol Abuse and Alcoholism. S.T. is a recipient of a pre-doctoral fellowship awarded by the Society for Neuroscience's Minority Neuroscience Fellowship Program.

References

- [1] T. Abel and E. Kandel, Positive and negative regulatory mechanisms that mediate long-term memory storage, *Brain Res. Brain Res. Rev.* **26** (1998), 360–378.
- [2] E. Adamec, P.S. Mohan, A.M. Cataldo, J.P. Vonsattel and R.A. Nixon, Up-regulation of the lysosomal system in experimental models of neuronal injury: implications for Alzheimer's disease, *Neuroscience* **100** (2000), 663–675.
- [3] K.T. Akama and L.J. Van Eldik, Beta-amyloid stimulation of inducible nitric-oxide synthase in astrocytes is interleukin-1 β - and tumor necrosis factor- α (TNF α)-dependent, and involves a TNF α receptor-associated factor- and NF κ B-inducing kinase-dependent signaling mechanism, *J. Biol. Chem.* **275** (2000), 7918–7924.
- [4] M.Y. Aksenov, M.V. Aksenova, D.A. Butterfield, J.W. Geddes and W.R. Markesbery, Protein oxidation in the brain in Alzheimer's disease, *Neuroscience* **103** (2001), 373–383.
- [5] A.P. Braun and H. Schulman, The multifunctional calcium/calmodulin-dependent protein kinase: from form to function, *Annu. Rev. Physiol.* **57** (1995), 417–445.
- [6] A. Castegna, M. Aksenov, M. Aksenova, V. Thongboonkerd, J.B. Klein, W.M. Pierce, R. Booze, W.R. Markesbery and D.A. Butterfield, Proteomic identification of oxidatively modified proteins in Alzheimer's disease brain. Part I: creatine kinase BB, glutamine synthase, and ubiquitin carboxy-terminal hydrolase L-1, *Free Radic. Biol. Med.* **33** (2002), 562–571.

- [7] A. Castegna, M. Aksenov, V. Thongboonkerd, J.B. Klein, W.M. Pierce, R. Booze, W.R. Markesbery and D.A. Butterfield, Proteomic identification of oxidatively modified proteins in Alzheimer's disease brain. Part II: dihydropyrimidinase-related protein 2, alpha-enolase and heat shock cognate 71, *J. Neurochem.* **82** (2002), 1524–1532.
- [8] S.L. Chan, K. Furukawa and M.P. Mattson, Presenilins and APP in neuritic and synaptic plasticity: implications for the pathogenesis of Alzheimer's disease, *Neuromolecular Med* **2** (2002), 167–196.
- [9] V.L. Dawson and T.M. Dawson, Nitric oxide in neurodegeneration, *Prog. Brain Res.* **118** (1998), 215–229.
- [10] P. De Koninck and H. Schulman, Sensitivity of CaM kinase II to the frequency of Ca²⁺ oscillations, *Science* **279** (1998), 227–230.
- [11] P. Eikelenboom and W.A. van Gool, Neuroinflammatory perspectives on the two faces of Alzheimer's disease, *J. Neural Transm.* **111** (2004), 281–294.
- [12] F.S. Espindola, E.M. Espreafico, M.V. Coelho, A.R. Martins, F.R. Costa, M.S. Mooseker and R.E. Larson, Biochemical and immunological characterization of p190-calmodulin complex from vertebrate brain: a novel calmodulin-binding myosin, *J. Cell Biol.* **118** (1992), 359–368.
- [13] H. Fillit, W.H. Ding, L. Buee, J. Kalman, L. Altstiel, B. Lawlor and G. Wolf-Klein, Elevated circulating tumor necrosis factor levels in Alzheimer's disease, *Neurosci. Lett.* **129** (1991), 318–320.
- [14] K.P. Giese, N.B. Fedorov, R.K. Filipkowski and A.J. Silva, Autophosphorylation at Thr286 of the alpha calcium-calmodulin kinase II in LTP and learning, *Science* **279** (1998), 870–873.
- [15] P. Grammas and R. Ovase, Inflammatory factors are elevated in brain microvessels in Alzheimer's disease, *Neurobiol. Aging* **22** (2001), 837–842.
- [16] W.S. Griffin, J.G. Sheng, M.C. Royston, S.M. Gentleman, J.E. McKenzie, D.I. Graham, G.W. Roberts and R.E. Mraz, Glial-neuronal interactions in Alzheimer's disease: the potential role of a cytokine cycle in disease progression, *Brain Pathol* **8** (1998), 65–72.
- [17] P.I. Hanson and H. Schulman, Neuronal Ca²⁺/calmodulin-dependent protein kinases, *Annu. Rev. Biochem.* **61** (1992), 559–601.
- [18] K. Hensley, N. Hall, R. Subramaniam, P. Cole, M. Harris, M. Aksenov, M. Aksenova, S.P. Gabbita, J.F. Wu, J.M. Carney, M. Lovell, W.R. Markesbery and D.A. Butterfield, Brain regional correspondence between Alzheimer's disease histopathology and biomarkers of protein oxidation, *J. Neurochem.* **65** (1995), 2146–2156.
- [19] L. Holcomb, M.N. Gordon, E. McGowan, X. Yu, S. Benkovic, P. Jantzen, K. Wright, I. Saad, R. Mueller, D. Morgan, S. Sanders, C. Zehr, K. O'Campo, J. Hardy, C.M. Prada, C. Eckman, S. Younkin, K. Hsiao and K. Duff, Accelerated Alzheimer-type phenotype in transgenic mice carrying both mutant amyloid precursor protein and presenilin 1 transgenes, *Nat. Med.* **4** (1998), 97–100.
- [20] E.R. Kandel, The molecular biology of memory storage: a dialog between genes and synapses, *Biosci. Rep.* **21** (2001), 565–611.
- [21] A. Keller, A.I. Nesvizhskii, E. Kolker and R. Aebersold, Empirical statistical model to estimate the accuracy of peptide identifications made by MS/MS and database search, *Anal. Chem.* **74** (2002), 5383–5392.
- [22] M.A. Korolainen, G. Goldsteins, I. Alafuzoff, J. Koistinaho and T. Pirttila, Proteomic analysis of protein oxidation in Alzheimer's disease brain, *Electrophoresis* **23** (2002), 3428–3433.
- [23] S.C. Lee, M.L. Zhao, A. Hirano and D.W. Dickson, Inducible nitric oxide synthase immunoreactivity in the Alzheimer disease hippocampus: association with Hirano bodies, neurofibrillary tangles, and senile plaques, *J. Neuropathol. Exp. Neurol.* **58** (1999), 1163–1169.
- [24] B.E. Lonze and D.D. Ginty, Function and regulation of CREB family transcription factors in the nervous system, *Neuron* **35** (2002), 605–623.
- [25] R.J. Mark, M.A. Lovell, W.R. Markesbery, K. Uchida and M.P. Mattson, A role for 4-hydroxynonenal, an aldehydic product of lipid peroxidation, in disruption of ion homeostasis and neuronal death induced by amyloid beta-peptide, *J. Neurochem.* **68** (1997), 255–264.
- [26] Y. Matsuoka, M. Picciano, J. La Francois and K. Duff, Fibrillar beta-amyloid evokes oxidative damage in a transgenic mouse model of Alzheimer's disease, *Neuroscience* **104** (2001), 609–613.
- [27] Y. Matsuoka, M. Picciano, B. Malester, J. LaFrancois, C. Zehr, J.M. Daeschner, J.A. Olschowka, M.I. Fonseca, M.K. O'Banion, A.J. Tenner, C.A. Lemere and K. Duff, Inflammatory responses to amyloidosis in a transgenic mouse model of Alzheimer's disease, *Am. J. Pathol.* **158** (2001), 1345–1354.
- [28] M. Mayford, M.E. Bach, Y.Y. Huang, L. Wang, R.D. Hawkins and E.R. Kandel, Control of memory formation through regulated expression of a CaMKII transgene, *Science* **274** (1996), 1678–1683.
- [29] A.I. Nesvizhskii, A. Keller, E. Kolker and R. Aebersold, A statistical model for identifying proteins by tandem mass spectrometry, *Anal. Chem.* **75** (2003), 4646–4658.
- [30] R.A. Nixon, A.M. Cataldo and P.M. Mathews, The endosomal-lysosomal system of neurons in Alzheimer's disease pathogenesis: a review, *Neurochem. Res.* **25** (2000), 1161–1172.
- [31] A. Nunomura, G. Perry, M.A. Pappolla, R. Wade, K. Hirai, S. Chiba and M.A. Smith, RNA oxidation is a prominent feature of vulnerable neurons in Alzheimer's disease, *J. Neurosci.* **19** (1999), 1959–1964.
- [32] G. Perry, A. Nunomura, K. Hirai, X. Zhu, M. Prez, J. Avila, R.J. Castellani, C.S. Atwood, G. Aliev, L.M. Sayre, A. Takeda and M.A. Smith, Is oxidative damage the fundamental pathogenic mechanism of Alzheimer's and other neurodegenerative diseases? *Free Radic. Biol. Med.* **33** (2002), 1475–1479.
- [33] M.J. Picklo, T.J. Montine, V. Amarnath and M.D. Neely, Carbonyl toxicology and Alzheimer's disease, *Toxicol. Appl. Pharmacol.* **184** (2002), 187–197.
- [34] K. Resing, K. Meyer-Arendt, A.M. Mendoza, L.D. Aveline-Wolf, K.R. Jonscher, K.G. Pierce, W.M. Old, H.T. Cheung, S. Russell, J.L. Wattawa, G.R. Goehle, R.D. Knight and N.G. Ahn, Improving reproducibility and sensitivity in identifying human proteins by shotgun proteomics, *Anal. Chem.* **76** (2004), 3556–3568.
- [35] L.M. Sayre, D.A. Zelasko, P.L. Harris, G. Perry, R.G. Salomon and M.A. Smith, 4-Hydroxynonenal-derived advanced lipid peroxidation end products are increased in Alzheimer's disease, *J. Neurochem.* **68** (1997), 2092–2097.
- [36] C.D. Smith, J.M. Carney, T. Tatsumo, E.R. Stadtman, R.A. Floyd and W.R. Markesbery, Protein oxidation in aging brain, *Ann. N.Y. Acad. Sci.* **663** (1992), 110–119.
- [37] M.A. Smith, P.L. Richey Harris, L.M. Sayre, J.S. Beckman and G. Perry, Widespread peroxy-nitrite-mediated damage in Alzheimer's disease, *J. Neurosci.* **17** (1997), 2653–2657.

- [38] M.A. Smith, P.L. Richey, S. Taneda, R.K. Kutty, L.M. Sayre, V.M. Monnier and G. Perry, Advanced Maillard reaction end products, free radicals, and protein oxidation in Alzheimer's disease, *Ann. N. Y. Acad. Sci.* **738** (1994), 447–454.
- [39] M.A. Smith, C.A. Rottkamp, A. Nunomura, A.K. Raina and G. Perry, Oxidative stress in Alzheimer's disease, *Biochim. Biophys. Acta* **1502** (2000), 139–144.
- [40] B.A. Soreghan, F. Yang, S.N. Thomas, J. Hsu and A.J. Yang, High-throughput proteomic-based identification of oxidatively induced protein carbonylation in mouse brain, *Pharm. Res.* **20** (2003), 1713–1720.
- [41] Y. Su, R.J. Balice-Gordon, D.M. Hess, D.S. Landsman, J. Minarcik, J. Golden, I. Hurwitz, S.A. Liebhaber and N.E. Cooke, Neurobeachin is essential for neuromuscular synaptic transmission, *J. Neurosci.* **24** (2004), 3627–3636.
- [42] C. Tan, A. Mui and S. Dedhar, Integrin-linked kinase regulates inducible nitric oxide synthase and cyclooxygenase-2 expression in an NF-kappa B-dependent manner, *J. Biol. Chem.* **277** (2002), 3109–3116.
- [43] R.S. Walikonis, O.N. Jensen, M. Mann, D.W. Provnance, Jr., J.A. Mercer and M.B. Kennedy, Identification of proteins in the postsynaptic density fraction by mass spectrometry, *J. Neurosci.* **20** (2000), 4069–4080.
- [44] X. Wang, F.W. Herberg, M.M. Laue, C. Wullner, B. Hu, E. Petrasch-Parwez and M.W. Kilimann, Neurobeachin: A protein kinase A-anchoring, beige/Chediak-higashi protein homolog implicated in neuronal membrane traffic, *J. Neurosci.* **20** (2000), 8551–8565.
- [45] T. Wataya, A. Nunomura, M.A. Smith, S.L. Siedlak, P.L. Harris, S. Shimohama, L.I. Szewda, M.A. Kaminski, J. Avila, D.L. Price, D.W. Cleveland, L.M. Sayre and G. Perry, High molecular weight neurofilament proteins are physiological substrates of adduction by the lipid peroxidation product hydroxynonenal, *J. Biol. Chem.* **277** (2002), 4644–4648.
- [46] Y.H. Wei and H.C. Lee, Oxidative stress, mitochondrial DNA mutation, and impairment of antioxidant enzymes in aging, *Exp. Biol. Med. (Maywood)* **227** (2002), 671–682.
- [47] D.A. Wolters, M.P. Washburn and J.R. Yates, An automated multidimensional protein identification technology for shotgun proteomics, *Anal. Chem.* **73** (2001), 5683–5690.
- [48] N. Yuri, S. Elkins, T. Nikolskaya and B. Andrej, A novel method for generation of signature networks as biomarkers from complex high throughput data, *Toxicol. Lett.* (2005), doi:10.1016/j.toxlet.2005.02.004.
- [49] S.H. Zuckerman, J. Gustin and G.F. Evans, Expression of CD54 (intercellular adhesion molecule-1) and the beta 1 integrin CD29 is modulated by a cyclic AMP dependent pathway in activated primary rat microglial cell cultures, *Inflamm.* **22** (1998), 95–106.